Proc. Camb. Phil. Soc. (1967), **63**, 827
PCPS 63–96
With 9 text-figures
Printed in Great Britain

Reflected and diffracted fields within a medium formed by a circular cylinder and two planes

By TAPENDRA NATH MAULIK
Bengal Engineering College, India

(*Received* 13 *April* 1966)

Abstract. Green's function for *SH*-line source inside a wedge shaped medium with its apex removed by a circular cylindrical surface has been obtained. Exact location of the image sources facilitates the determination of the reflexion and diffraction at the circular and also at the plane boundary of the multiple phases clearly. The scattered field from the corner is indicated. The connexion of this solution with that of complete wedge has been shown with suitable contour integrations.

1. *Introduction.* Many papers have been devoted to the problem of reflexion and diffraction of waves by a wedge since the original study of Macdonald (7). Because of its inherent general character and wide applicability in Physics it has received the attention of many, and they applied different mathematical disciplines to picture the complete description of the disturbed field starting with a different incident field and with various types of boundary conditions. For a good bibliography of the earlier works one may consult Oberhettinger (8). He showed that the problem of finding the resultant field would be comparatively simpler by assuming the incident field in a suitable form. Hudson (4) used these techniques for seismic wave propagation within a wedge and discussed the image system in detail. He further extended the solution for a harmonic source to find the solution due to an *SH*-pulse, and also estimated the Love wave generated.

Wave propagation inside or outside a wedge has a special importance in seismology in relation to the continental margin and different curved margins inside the earth. The purpose of this paper is to consider a more complex geometry which will have a direct application to the mountain root problem. But the calculation permitting both *P* and *S* waves in elastic wedge is highly involved even when the wedge is complete. We are therefore considering the propagation of the *SH*-wave due to a line source, but in a more complex geometry, namely in the convex part of the medium formed by the circular cylinder of arbitrary radius and two planes. The image system explained by Hudson, mentioned earlier, is found to be very useful for geometrical interpretation and the same has been followed here. For a complete wedge Oberhettinger (8) or Hudson (4) had to start with a suitable form of the whole field involving two arbitrary constants, to fit the prescribed boundary conditions on the plane boundaries. On the contrary, we have obtained a direct solution of the given differential equation under

https://doi.org/10.1017/S0305004100041815 Published online by Cambridge University Press

prescribed boundary conditions following Cohen(1) and Sommerfeld(9) as the sum of a set of eigenfunctions, and it is possible since the apex of the wedge is removed (and thereby bringing two apices!) by a circular cylinder. The success of the method lies in separating the involved variables of the given partial differential equations, when a set of functions satisfying the prescribed condition on a part of the boundary, and the given differential equation, is chosen. The solution thus obtained will be obviously a summation over some characteristic values. In the next part of our work we shall give:

(i) different representations of the solution by contour integrations,

(ii) identify different components of the wave, i.e. reflected waves, diffracted waves, etc., by separating out the different terms. In doing so the image system has been further generalized and expressed in a single formula and that enables us to give a proper ray-picture with usual short-wave approximation. The introduction of the circular cylinder between the two planes helps us on one side to solve the problem directly, while on the other brings with it the complex wave pattern due to its presence.

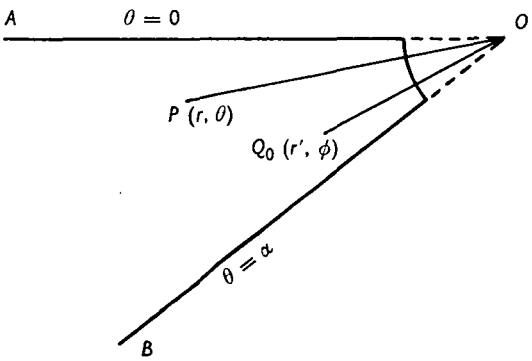


Fig. 1. The line source Q_0 and the observer P in the medium.

For a given value of the wedge angle and given source, the image sources are once for all fixed and the field for a complete wedge is not difficult to determine, and in fact has been discussed in detail in earlier works. But in our case the field is further dependent on the position of the observer. If the observer is nearer the cylindrical surface he will get more reflected and diffracted waves from the cylindrical boundary than when he will be far away from it. This problem has been solved by the introduction of the idea of the 'shadow zone of the images'.

2. *Formal method of solution.* Consider a line source situated parallel to the edge of a nearly wedge-shaped medium as shown in Figure 1. Let α be the arbitrary angle of the wedge, and let the apex of the wedge be indented by a circular cylindrical surface of arbitrary radius a. Let (r', ϕ) be the source point and (r, θ) be the observing point. Then if we assume the field within this medium be harmonic in time then the displacement

$$u = \Psi(r, \theta) \exp\{\pm i\omega t\}, \tag{2·1}$$

where Ψ satisfies

$$\nabla^2\Psi + k^2\Psi = f(r, \theta) \quad (r > a) \tag{2·2}$$

and $k = \omega/\beta$, β being the velocity of propagation of waves through the medium, $f(r, \theta)$ is the source function.

https://doi.org/10.1017/S0305004100041815 Published online by Cambridge University Press

Conditions on the three boundaries $\theta = 0$, $\theta = \alpha$, $r = a$ may be assumed in various ways along with mixed condition on the cylindrical boundary. Let G be the appropriate Green's function in the convex part of the medium (i.e. $0 < \theta < \alpha, r > a$, cf. Figure 1). Obviously, G will satisfy

$$\frac{\partial^2 G}{\partial r^2}+\frac{1}{r}\frac{\partial G}{\partial r}+\frac{1}{r^2}\frac{\partial^2 G}{\partial \theta^2}+k^2 G = -\frac{4\pi}{r}\delta(r-r')\,\delta(\theta-\phi) \tag{2·3}$$

save for the time factor $\exp\{\pm i\omega t\}$.

If we assume the boundary $r = a$ as free, $\partial G/\partial r = 0$ on $r = a$ and if it is rigid then $G = 0$ on $r = a$. Thus if we take the r-dependent part of G as $H_\nu^{(1)}(kr)$, where $H_\nu^{(1)}(kr)$ is the first kind of Hankel function (in this case we have to choose $\exp\{-i\omega t\}$ for diverging waves from the source) we have to select ν's satisfying

$$\text{(i)}\quad H_\nu^{(1)}(kr)\big|_{r=a} = H_\nu^{(1)}(ka) = 0 \quad \text{if} \quad G = 0 \quad \text{on} \quad r = a \quad \text{for all } \theta, \tag{2·4}$$

$$\text{(ii)}\quad \dot{H}_\nu^{(1)}(kr)\big|_{r=a} = \eta_\nu^{(1)}(ka) = 0 \quad \text{if} \quad \frac{\partial G}{\partial r} = 0 \quad \text{on} \quad r = a \quad \text{for all } \theta. \tag{2·5}$$

Here a dot denotes the differentiation with reference to its argument. It has been shown by Magnus and Cotin (cf. Cohen(1)) and by Sommerfeld(9), p. 122, that $H_\nu^{(1)}(ka)$ has a denumerable number of simple zeros which lie on the first and third quadrant of the complex ν-plane. Sommerfeld using the method of steepest descent showed that the zeros are given by

$$\nu_n = ka + \tfrac{1}{2}(ka)^{\frac{1}{3}}[\tfrac{3}{4}\pi(4n-1)]^{\frac{2}{3}} e^{\frac{1}{3}i\pi} \quad (n = 1, 2, 3, \ldots), \tag{2·6}$$

in the positive quadrant of the ν-plane. On the other hand Magnus and Cotin expressed these values of ν_n in the form $\alpha_n + i\beta_n$, and which will be helpful for computational purposes. The zeros of $\eta_\nu^{(1)}(ka)$ can also be found in the same way. In fact if one applies the method of steepest descent then these zeros are (cf. Duwalo and Jacobs(2) or Figure 3)

$$\nu_n = ka + \tfrac{1}{2}(ka)^{\frac{1}{3}}[\tfrac{3}{4}\pi(4n+1)]^{\frac{2}{3}} e^{\frac{1}{3}i\pi} \quad (n = 0, 1, 2, \ldots). \tag{2·7}$$

Writing G in the form

$$G = \sum_n c_n(\theta)\, H_{\nu_n}^{(1)}(kr), \tag{2·8}$$

where ν_n are the denumerable zeros of $H_\nu^{(1)}(ka)$ or $\eta_\nu^{(1)}(ka)$ which lie on the first quadrant of the complex ν-plane and according as the boundary $r = a$ is rigid or weak. It can easily be verified that (2·8) satisfies the Sommerfeld's radiation condition

$$\lim_{r\to\infty}\left|r^{\frac{1}{2}}\left(\frac{\partial G}{\partial r} - ikG\right)\right| = 0. \tag{2·9}$$

Substituting (2·8) in (2·3) we get

$$\sum_n [c_n''(\theta) + \nu_n^2 c_n(\theta)]\frac{1}{r} H_{\nu_n}^{(1)}(kr) = -4\pi\delta(r-r')\,\delta(\theta-\phi).$$

Multiplying both sides by $H_{\nu_n}^{(1)}(kr)$ and integrating from a to ∞ and assuming the validity of the interchange of the summation and integral, which may be seen to be true, we get

$$c_n''(\theta) + \nu_n^2 c_n(\theta) = A_n\,\delta(\theta-\phi) \tag{2·10}$$

https://doi.org/10.1017/S0305004100041815 Published online by Cambridge University Press

because of the orthogonal property

$$\int_a^\infty H_{\nu_n}^{(1)}(kr)\, H_{\nu_m}^{(1)}(kr)\frac{dr}{r} = N_{nm}\,\delta_{nm}, \tag{2·11}$$

where δ_{nm} is the Kronecker δ symbol and

$$A_n = -\frac{4\pi H_{\nu_n}^{(1)}(kr')}{N_{nn}}, \tag{2·12}$$

$$N_{nn} = \left[\frac{2i}{\pi\nu}\frac{\partial/\partial\nu[H_\nu^{(1)}(kr)]}{H_\nu^{(2)}(kr)}\right]_{\substack{r=a\\ \nu=\nu_n}} \quad \text{(if the circular cylindrical boundary is rigid)}, \tag{2·13}$$

$$N_{nn} = \left[\frac{2i}{\pi\nu}\frac{\partial/\partial\nu[\eta_\nu^{(1)}(kr)]}{\eta_\nu^{(2)}(kr)}\right]_{\substack{r=a\\ \nu=\nu_n}} \quad \text{(if the circular cylindrical boundary is free)}. \tag{2·14}$$

The conditions on the plane boundaries may be chosen in various ways. But we are restricting only to three cases, since in these cases the operations will be almost identical and their corresponding complete wedge solutions are known. We select

$$\left.\begin{aligned} &(a)\ c_n(\theta) = 0, \quad \text{on} \quad \theta = 0 \quad \text{and} \quad \theta = \alpha;\\ &(b)\ c_n'(\theta) = 0, \quad \text{on} \quad \theta = 0 \quad \text{and} \quad \theta = \alpha;\\ &(c)\ c_n'(\theta) = 0, \quad \text{on} \quad \theta = 0 \quad \text{and} \quad c_n(\theta) = 0 \quad \text{on} \quad \theta = \alpha; \end{aligned}\right\} \tag{2·15}$$

prime denoting differentiation with respect to θ. For a complete wedge, Oberhettinger(8) considered the cases (a) and (b), and Hudson(4) (c). Solution of (2·10) under the set of boundary conditions (2·15) may be obtained after a little algebra in the form

$$c_n(\theta) = \frac{A_n}{2\nu_n \sin\nu_n\alpha}[\cos\nu_n(\alpha - |\theta-\phi|) - \cos\nu_n(\alpha - |\theta+\phi|)] \tag{2·16}$$

$$= \frac{A_n}{2\nu_n \sin\nu_n\alpha}[\cos\nu_n(\alpha - |\theta-\phi|) + \cos\nu_n(\alpha - |\theta+\phi|)] \tag{2·17}$$

$$= -\frac{A_n}{2\nu_n \cos\nu_n\alpha}[\sin\nu_n(\alpha - |\theta-\phi|) + \sin\nu_n(\alpha - |\theta+\phi|)] \tag{2·18}$$

for all $\theta, \phi < \alpha$, except $\theta = \phi$.

It may be of interest to draw the attention to the fact that the θ-dependent part of our problem is the same as Oberhettinger's or Hudson's results. Substituting from (2·12), (2·13) and (2·16)–(2·18) in (2·8) we get the formal representation when $r = a$ is rigid as

$$G_j = \pi^2 i \sum_{n=1}^{\infty} \frac{H_{\nu_n}^{(2)}(ka)}{\partial/\partial\nu[H_\nu^{(1)}(ka)]_{\nu=\nu_n}} H_{\nu_n}^{(1)}(kr)\, H_{\nu_n}^{(1)}(kr')\, F_j(\nu_n) \quad (j = 1, 2, 3), \tag{2·19}$$

$$F_j(\nu_n) = \frac{\cos\nu_n(\alpha - \Phi_1) + (-1)^j \cos\nu_n(\alpha - \Phi_2)}{\sin\nu_n\alpha} \quad (j = 1, 2) \tag{2·20}$$

$$= -\frac{\sin\nu_n(\alpha - \Phi_1) + \sin\nu_n(\alpha - \Phi_2)}{\cos\nu_n\alpha} \quad (j = 3), \tag{2·21}$$

where

$$\Phi_1 = |\theta - \phi|, \quad \Phi_2 = |\theta + \phi|, \tag{2·22}$$

https://doi.org/10.1017/S0305004100041815 Published online by Cambridge University Press

if $r = a$ is weak then $H_{\nu_n}^{(2)}(ka)/(\partial/\partial\nu)\,[H_\nu^{(1)}(ka)]_{\nu=\nu_n}$ should be replaced by

$$\eta_\nu^{(2)}(ka)/(\partial/\partial\nu)\,[\eta_\nu^{(1)}(ka)]_{\nu=\nu_n},$$

where $\eta_\nu^{1,2}$ are defined in (2·5). The convergence of the expansion (2·19) over the complex zeros of $H_\nu^{(1)}(ka)$ or $\eta_\nu^{(1)}(ka)$ is very rapid (cf. Sommerfeld(9), p. 289).

3. *Transformation of the formal solution.* The Green's function has been obtained in the form of a summation in (2·19). That the result is equivalent to two alternative forms will be explained in section 3. For this purpose we select two integrals along two different contours Γ_1 and Γ_2 as

$$\int_{\Gamma_1} \frac{J_\nu(ka)}{H_\nu^{(1)}(ka)} H_\nu^{(1)}(kr)\, H_\nu^{(1)}(kr')\, F_j(\nu)\, d\nu \quad (j = 1, 2), \tag{3·1}$$

where Γ_1 is a contour in the right half of the complex ν-plane consisting of four parts:

(i) a line parallel to the imaginary axis from $i\infty$ to $i\delta$;

(ii) a small semi-circle of radius δ ($\delta \to 0+$);

(iii) the line $-i\delta$ to $-i\infty$;

(iv) a large semi-circle of radius $R = (N + \frac{1}{2})\,\pi/\alpha$, N being a large positive integer; and

$$\int_{\Gamma_2} \frac{J_\nu(ka)}{H_\nu^{(1)}(ka)} H_\nu^{(1)}(kr)\, H_\nu^{(1)}(kr')\, F_j(\nu)\, d\nu \quad (j = 1, 2), \tag{3·2}$$

where Γ_2 is a contour consisting of the following parts in the right half of the complex ν-plane:

(i) the imaginary axis from $i\infty$ to $i\delta_0$;

(ii) a quarter of a small circle of radius $i\delta_0$ ($\delta_0 \to 0+$);

(iii) the real axis half encircled at each zero of $\sin\nu\alpha$ (i.e. at $\nu_r = r\pi/\alpha, r = 1, 2, \ldots$) by small semi-circles of radii δ_r, such that $\delta \to 0$, δ being the norm of δ_r;

(iv) a large quarter of a circle of radius $R = (N + \frac{1}{2})\,\pi/\alpha$, N being a large positive integer. To find the condition under which the integrals converge and tend to zero on the infinite circles we write, using Stirling's formula,

$$\Gamma(\nu) = \sqrt{2\pi}\, e^{-\nu} \nu^{\nu - \frac{1}{2}} \quad (-\pi < \arg\nu < \pi),$$

$$J_\nu(z) = (\tfrac{1}{2}z)^\nu \left[\frac{1}{\Gamma(\nu+1)} - \frac{(\frac{1}{2}z)^2}{\Gamma(\nu+2)} + \ldots\right]$$

$$\approx \frac{1}{\sqrt{(2\pi\nu)}} \mu^{-\nu} \quad \text{as} \quad |\nu| \to \infty, \{\Re\nu\} > 0, \tag{3·3}$$

where

$$\mu = 2\nu/ze. \tag{3·4}$$

Similarly when $\{\Re\nu\} > 0$ and $|\nu| \to \infty$ we have

$$J_{-\nu}(z) \approx \frac{2}{\sqrt{(2\pi\nu)}} \sin\pi\nu\mu^\nu,$$

and

$$H_\nu^{(1)}(z) \approx \frac{2}{\sqrt{(2\pi\nu)}} \left[\mu^\nu - \frac{e^{-i\pi\nu}}{2\sin\pi\nu} \mu^{-\nu}\right]. \tag{3·5}$$

https://doi.org/10.1017/S0305004100041815 Published online by Cambridge University Press

Using equation (3·2) through (3·5), we get

$$\frac{H_\nu^{(1)}(kr)}{H_\nu^{(1)}(ka)} \approx \text{const.} \left(\frac{a}{r}\right)^\nu \quad \text{as} \quad |\nu| \to \infty, \tag{3·6}$$

$$H_\nu^{(1)}(kr') J_\nu(ka) \approx \text{const.} \frac{1}{\pi\nu} \left(\frac{a}{r'}\right)^\nu \quad \text{as} \quad |\nu| \to \infty. \tag{3·7}$$

Again writing $\nu = \sigma + i\tau$, with $\{\Re\nu\} > 0$ and

$$E(\nu) = \left|\frac{\cos\nu(\alpha - \Phi)}{\sin\nu\alpha}\right| \tag{3·8}$$

we get

$$E(\tau) = \frac{e^{-\tau(\alpha-\Phi)} + e^{\tau(\alpha-\Phi)}}{e^{-\tau\alpha} - e^{\tau\alpha}}. \tag{3·9}$$

Hence if $\{\Im\nu\} > 0$, then $\lim_{\tau\to\infty} E(\tau) \to 0$ if $0 < \Phi < 2\alpha$. (3·10)

Since

$$E(-\tau) = E(\tau) \tag{3·11}$$

we get the same result for $\{\Im\nu\} < 0$. Combining the conditions (3·6), (3·7), (3·10) and (3·11) we note that if

$$r > a, \quad r' > a, \quad 0 < \Phi_1 < \alpha, \quad 0 < \Phi_2 < 2\alpha, \tag{3·12}$$

the integral on the infinite arc converges to zero. The first two conditions are easily satisfied since we are considering the convex part of the boundaries but the implication of the second two results are that the solution will diverge on $\theta = \phi$ ($\Phi_1 = 0$).

Hence performing the integration given in (3·1) we get

$$L_j = -T_j + I_j^P \quad (j = 1, 2), \tag{3·13}$$

where

$$L_j = 2\pi i \sum_{n=1}^{\infty} Q_{\nu_n} F_j(\nu_n), \tag{3·14}$$

$$T_j = \frac{2\pi i}{\alpha} \sum_{n=0}^{\infty} \epsilon_n Q_{n\pi/\alpha} \left[\cos\frac{n\pi}{\alpha}\Phi_1 + (-1)^j \cos\frac{n\pi}{\alpha}\Phi_2\right] \tag{3·15}$$

and

$$I_j^p = \int_{i\infty}^{-i\infty} Q_\nu F_j(\nu)\, d\nu = \int_0^{i\infty} (Q_{-\nu} - Q_\nu) F_j(\nu)\, d\nu, \tag{3·16}$$

$$Q_\nu = \frac{J_\nu(ka)}{H_\nu^{(1)}(ka)} H_\nu^{(1)}(kr) H_\nu^{(1)}(kr'), \tag{3·17}$$

$$Q'_{\nu_n} = \frac{J_{\nu_n}(ka)}{\partial/\partial\nu[H_\nu^{(1)}(ka)]_{\nu=\nu_n}} H_{\nu_n}^{(1)}(kr) H_{\nu_n}^{(1)}(kr'), \tag{3·18}$$

$$\left.\begin{aligned} \epsilon_n &= \tfrac{1}{2} \quad \text{for} \quad n = 0, \\ &= 1 \quad \text{for} \quad n \geqslant 1. \end{aligned}\right\} \tag{3·19}$$

However, using

$$H_{-\nu}^{(1)}(z) = e^{i\nu\pi} H_\nu^{(1)}(z) \tag{3·20}$$

and

$$H_\nu^{(1)}(z) = \frac{J_{-\nu}(z) - e^{-i\nu\pi} J_\nu(z)}{i \sin\nu\pi} \tag{3·21}$$

we shall get

$$Q_{-\nu} - Q_\nu = i \sin\nu\pi H_\nu^{(1)}(kr) H_\nu^{(1)}(kr') e^{i\nu\pi} \tag{3·22}$$

https://doi.org/10.1017/S0305004100041815 Published online by Cambridge University Press

and hence
$$I_j^P = i\int_0^{i\infty} H_\nu^{(1)}(kr)\,H_\nu^{(1)}(kr')\sin\nu\pi\, e^{i\nu\pi}F_j(\nu)\,d\nu. \tag{3·23}$$

For the circumstances postulated above we can perform the integration given in (3·2) and on integration we get
$$L_j = -\tfrac{1}{2}T_j - I_j^Q + I_j^R, \tag{3·24}$$

where
$$I_j^Q = \int_0^{i\infty} Q_\nu F_j(\nu)\,d\nu, \tag{3·25}$$

$$I_j^R = \int_0^{\infty} Q_\nu F_j(\nu)\,d\nu \quad (j=1,2). \tag{3·26}$$

This has been done to use the fact that the zeros of $H_\nu^{(1)}(ka)$ are on the positive quadrant only in the right half of the complex ν-plane

$$T_j = \frac{2\pi i}{\alpha}\sum_{n=0}^{\infty}{}'\,\epsilon_n \frac{J_{n\pi/\alpha}(ka)}{H^{(1)}_{n\pi/\alpha}(ka)}\,H^{(1)}_{n\pi/\alpha}(kr)\,H^{(1)}_{n\pi/\alpha}(kr')\left[\cos\frac{n\pi}{\alpha}\Phi_1 + (-1)^j\cos\frac{n\pi}{\alpha}\Phi_2\right]. \tag{3·27}$$

When $r > r'$ we write
$$H^{(1)}_{n\pi/\alpha}(kr') = 2J_{n\pi/\alpha}(kr') - H^{(2)}_{n\pi/\alpha}(kr') \tag{3·28}$$

and after some calculation

$$\begin{aligned} T_j = {} & \frac{2\pi i}{\alpha}\sum_{n=0}^{\infty}{}'\,\epsilon_n H^{(1)}_{n\pi/\alpha}(kr)\,J_{n\pi/\alpha}(kr')\left[\cos\frac{n\pi}{\alpha}\Phi_1 + (-1)^j\cos\frac{n\pi}{\alpha}\Phi_2\right] \\ & - \frac{2\pi i}{\alpha}\sum_{n=0}^{\infty}{}'\,\epsilon_n\left[H^{(2)}_{n\pi/\alpha}(kr')\,J_{n\pi/\alpha}(ka) - H^{(2)}_{n\pi/\alpha}(ka)\,J_{n\pi/\alpha}(kr')\right] \\ & \times \frac{H^{(1)}_{n\pi/\alpha}(kr)}{H^{(1)}_{n\pi/\alpha}(ka)}\left[\cos\frac{n\pi}{\alpha}\Phi_1 + (-1)^j\cos\frac{n\pi}{\alpha}\Phi_2\right] \quad (r > r', j = 1,2), \end{aligned} \tag{3·29}$$

when $r < r'$, r and r' are to be interchanged. It may be noted that in T_j, $\theta \gtrless \phi$ has no effect, i.e. singularity on $\theta = \phi$ is transferred to $r = r'$. The first term is easily shown to be equal to I_j^P, comparing a result of Oberhettinger(8) or a simpler proof may be constructed as follows. Consider the integral for $r > r'$

$$\int_{\Gamma_1} H_\nu^{(1)}(kr)\,J_\nu(kr')\,F_j(\nu)\,d\nu, \tag{3·30}$$

where Γ_1 is defined above. Also from (3·3) and (3·5)

$$H_\nu^{(1)}(kr)\,J_\nu(kr') \approx \text{const.}\frac{1}{\pi\nu}\left(\frac{r'}{r}\right)^\nu \quad \text{as} \quad |\nu| \to \infty,\ \{\Re\nu\} > 0 \to 0 \quad \text{if} \quad r > r'; \tag{3·31}$$

restrictions on Φ_1 and Φ_2 remain the same as in (3·12), and as such performing the integration

$$I_j^P = \frac{2\pi i}{\alpha}\sum_{n=0}^{\infty}{}'\,\epsilon_n H^{(1)}_{n\pi/\alpha}(kr)\,J_{n\pi/\alpha}(kr')\left[\cos\frac{n\pi}{\alpha}\Phi_1 + (-1)^j\cos\frac{n\pi}{\alpha}\Phi_2\right] \quad (j=1,2). \tag{3·32}$$

This I_j^P is easily seen to be the total field due to a source within a complete wedge under the similar boundary conditions on the plane boundaries, proceeding exactly in a similar manner as Oberhettinger(8), we get

$$T_j = I_j^P - S_j \quad (j=1,2), \tag{3·33}$$

https://doi.org/10.1017/S0305004100041815 Published online by Cambridge University Press

where S_j is given by the second term of (3·29). Hence from (3·13), (3·24) and (3·33) we get

$$L_j = S_j$$
$$= -I_j^P - 2I_j^Q + 2I_j^R \quad (j = 1, 2). \tag{3·34}$$

Comparing (2·19) and (3·14) and noting that at the zeros $H_{\nu_n}^{(1)}(ka) + H_{\nu_n}^{(2)}(ka) = 2J_{\nu_n}(ka)$ we get

$$G_j = \pi^2 i \sum_{n=1}^{\infty} \frac{H_{\nu_n}^{(2)}(ka)}{\partial/\partial\nu[H_\nu^{(1)}(ka)]_{\nu=\nu_n}} H_{\nu_n}^{(1)}(kr)\, H_{\nu_n}^{(1)}(kr')\, F_j(\nu_n)$$
$$(j = 1, 2; 0 < \Phi_1 < \alpha,\ 0 < \Phi_2 < 2\alpha). \tag{3·35}$$

This is equivalent to

$$G_j = -\pi i \int_0^{i\infty} H_\nu^{(1)}(kr)\, H_\nu^{(1)}(kr')\, e^{i\nu\pi} \sin \nu\pi\, F_j(\nu)\, d\nu$$
$$- 2\pi \int_0^{i\infty} \frac{J_\nu(ka)}{H_\nu^{(1)}(ka)} H_\nu^{(1)}(kr)\, H_\nu^{(1)}(kr')\, F_j(\nu)\, d\nu$$
$$+ 2\pi \int_0^{\infty} \frac{J_\nu(ka)}{H_\nu^{(1)}(ka)} H_\nu^{(1)}(kr)\, H_\nu^{(1)}(kr')\, F_j(\nu)\, d\nu \quad (j = 1, 2). \tag{3·36}$$

Both the representations (3·35) and (3·36) of Green's function contain singularity in the angular coordinate (i.e. at $\theta = \phi$). It is clear that πS_j (cf. (3·34) and (3·29)) is the alternative representation of G_j with singularity in the radial coordinate (i.e. at $r = r'$). One can easily show the convergency and also the rapidity of the convergency of (3·35) as $|\nu_n| \to \infty$ using the asymptotic values of ν_n in the form,

$$\nu_n \log\left(\frac{2\nu_n}{kae}\right) = (n - \tfrac{1}{4})\pi i \tag{3·37}$$

if n denotes a large integer (cf. Cohen (7)).

A similar calculation may be performed for $j = 3$ (corresponding to Hudson's case), and since here the poles on the real axis are those of $\cos \nu\alpha = 0$ the radii of large circles of Γ_1 and Γ_2 are to be taken as $N\pi/\alpha$, N being a large positive integer, instead of $(N + \frac{1}{2})\pi/\alpha$ as in the previous case for $j = 1, 2$ to avoid the singularities on the real axis. It will be seen that (3·35) and (3·36) will retain similar form but the representation corresponding to πS_j ($r \neq r'$) will be modified.

Instead of proceeding with the condition $G = 0$ on $r = a$ if we would start with $\partial G/\partial r = 0$ on $r = a$ then comparing (2·7) or Figure 3, it is clear that no modification is necessary for performing the integration along the described contours. Solution may be obtained from (3·35) and (3.36), by replacing $H_\nu^{(1)}(ka)$ and $H_\nu^{(2)}(ka)$ by $\eta_\nu^1(ka)$ and $\eta_\nu^{(2)}(ka)$. Also the summation over n is to be taken from 0 to ∞ instead of from 1 to ∞.

4. *Transformation of $F_j(\nu)$.* From the above it is now clear that for the representations (3·35) and (3·36) we can write $j = 1, 2, 3$. We shall now reduce $F_j(\nu)$ in a suitable form to distinguish the direct, reflected and diffracted waves. For that, we shall use the relation

$$\frac{\sin \zeta}{\sin \eta} = 2 \sum_{l=2}^{m} \cos[\zeta - (2l-1)\eta] - \frac{\sin(2m\eta - \zeta)}{\sin \eta}, \tag{4·1}$$

https://doi.org/10.1017/S0305004100041815 Published online by Cambridge University Press

where ζ and η will be respectively of the form X and Y and

$$\frac{\sin\zeta}{\sin\eta} = -2\sum_{l=1}^{m}\cos[\zeta+(2l-1)\eta]+\frac{\sin(2m\eta+\zeta)}{\sin\eta}, \tag{4·2}$$

where ζ, η will be of the form $(\frac{1}{2}\pi - X)$, Y or X, $(\frac{1}{2}\pi - Y)$ respectively.

Case I. $\alpha = \pi/m$, *where* m *is a positive integer.* Applying (4·1) we get

$$\frac{\sin\nu\pi}{\sin\nu\pi/m} = \sum_{l=1}^{m}\cos\frac{\nu\pi}{m}(m+1-2l). \tag{4·3}$$

So,

$$\frac{\sin\nu\pi\cos\nu(\alpha-\Phi_1)}{\sin\nu\pi/m} = \frac{1}{2}\sum_{l=1}^{m}\cos\nu\left[\pi-\frac{2\pi}{m}(l-1)-\Phi_1\right]+\frac{1}{2}\sum_{l=1}^{m}\cos\nu\left[\pi-\frac{2\pi l}{m}+\Phi_1\right]. \tag{4·4}$$

In the second summation replace l by $(m-l+1)$ and it is easy to verify that the first and second summations are equal and hence

$$\sin\nu\pi\,F_j(\nu) = \sum_{l=1}^{m}\cos\nu\left[\pi-\frac{2\pi}{m}(l-1)-\Phi_1\right] + (-1)^j\sum_{l=1}^{m}\cos\nu\left[\pi-\frac{2\pi}{m}l+\Phi_2\right] \quad (j=1,2). \tag{4·5}$$

Unfortunately for all $l = 1, 2, \ldots, m$, we cannot get a direct correspondence of l with the exact number of reflexion and so we shall rearrange (4·5) (see Appendix A) and write

$$F_2(\nu)\sin\nu\pi = \sum_{s=-m}^{m-1}\cos\nu(\pi-|\phi_s-\theta|), \tag{4·6}$$

where

$$\phi_s = \frac{\pi}{m}s+(-1)^s\phi+\frac{\pi}{m}\delta_s, \tag{4·7}$$

$$\phi_{-s} = 2\pi-\phi_{s-1} \tag{4·8}$$

and

$$\left.\begin{aligned}\delta_s &= 1 \text{ for } s \text{ being odd integer}\\ &= 0 \text{ for } s \text{ being even integer},\\ \delta_0 &= 0, \quad \delta_{-s} = \delta_s.\end{aligned}\right\} \tag{4·9}$$

Similarly

$$F_1(\nu)\sin\nu\pi = \sum_{s=-m}^{m-1}(-1)^s\cos\nu[\pi-|\phi_s-\theta|] \tag{4·10}$$

when ϕ_s is the same as before.

For $F_3(\nu)$ we have to use (4·2) and if $\alpha = \pi/n$ then

$$(1+\cos n\pi)\frac{\sin\nu\pi}{\cos\nu\pi/m} = 2\sum_{l=1}^{n}(-1)^l\sin\nu\pi\left[\frac{n+1-2l}{n}\right] \tag{4·11}$$

and hence if n is an odd integer the left-hand side is zero and if n is an even integer say $2m$ then

$$\frac{\sin\nu(\alpha-\Phi_1)\sin\nu\pi}{\cos\nu\pi/2m} = \sum_{1}^{2m}(-1)^l\cos\nu\left[\pi-\frac{\pi}{m}(l-1)-\Phi_1\right], \tag{4·12}$$

since

$$\sum_{1}^{2m}(-1)^{l-1}\cos\nu\left[-\pi+\frac{\pi l}{m}-\Phi_1\right] = \sum_{1}^{2m}(-1)^l\cos\nu\left[\pi-\frac{\pi}{m}(l-1)-\Phi_1\right]. \tag{4·13}$$

https://doi.org/10.1017/S0305004100041815 Published online by Cambridge University Press

Therefore
$$F_3(\nu)\sin\nu\pi = \sum_{1}^{2m}(-1)^{l-1}\cos\nu\left[\pi-\frac{\pi}{m}(l-1)-\Phi_1\right] + \sum_{1}^{2m}(-1)^{l-1}\cos\nu\left[\pi-\frac{\pi}{m}(l-1)-\Phi_2\right]. \tag{4·14}$$

However, (4·14) can be rearranged as in (4·6) and

$$F_3(\nu)\sin\nu\pi = \sum_{-2m}^{2m-1}(-1)^{\mu_s}\cos\nu[\pi-|\phi_s-\theta|]. \tag{4·15}$$

ϕ_s is the same as in (4·7)–(4·9) and

$$\mu_s = \tfrac{1}{2}(s+\delta_s). \tag{4·16}$$

Case II. If $\pi/m < \alpha < \pi/m - 1$ where m is an even or odd integer. In this case reduction is also straightforward (see Appendix A) and $F_j(\nu)$ can be reduced in the following form:

$$\sin\nu\pi\, F_j(\nu) = \sum_{-2m}^{m-1}(-1)^{sj}\cos\nu[\pi-|\phi_s-\theta|]+P_j\sin\nu\pi \quad (j=1,2), \tag{4·17}$$

where
$$\phi_s = s\alpha+(-1)^s\phi+\delta_s\alpha, \tag{4·18}$$

$$\phi_{-s} = 2\pi-\phi_{s-1}, \tag{4·19}$$

δ_s as defined in (4·9), and

$$P_j = \frac{\sin\nu(\pi-m\alpha)}{\sin\nu\pi\sin\nu\alpha}[\cos\nu(\alpha-\Phi_1)+(-1)^j\cos\nu(\alpha-\Phi_2)]$$

for m being an even integer, $j = 1, 2$, (4·20)

$$P_j = \frac{\sin\nu[\pi-(m+1)\alpha]\cos\nu(\alpha-\Phi_1)+(-1)^j\sin\nu[\pi-(m-1)\alpha]\cos\nu(\alpha-\Phi_2)}{\sin\nu\pi\sin\nu\alpha}$$

for m being an odd integer, $j = 1, 2$. (4·21)

Similarly using (4·2)

$$F_3(\nu)\sin\nu\pi = \sum_{-m}^{m-1}(-1)^{\mu_s}\cos\nu[\pi-|\phi_s-\theta|]+P_3\sin\nu\pi, \tag{4·22}$$

where
$$P_3 = \frac{(-1)^{m-1}\sin\nu(\pi-2m\alpha)[\sin\nu(\alpha-\Phi_1)+\sin\nu(\alpha-\Phi_2)]}{\sin\nu\pi\cos\nu\alpha}. \tag{4·23}$$

It is interesting to note that (4·18) and (4·19) is compatible with (4·7) and (4·8).

5. *Direct wave and the reflected waves from the plane boundary.* From the integral representation of G_j we note that the first term of (3·36) is

$$G_j' = -\pi i\int_0^{i\infty} H_\nu^{(1)}(kr)\,H_\nu^{(1)}(kr')\,e^{i\nu\pi}\sin\nu\pi\,F_j(\nu)\,d\nu \quad (j=1,2,3). \tag{5·1}$$

In section 3 we have noted that G_j' corresponds to the Green's function for a complete wedge under similar boundary conditions as in (2·15). Using (4·17) and (4·22) we get

$$G_j' = \sum_{s=-m}^{m-1}B_s^j W(\phi_s)+D_j \quad (j=1,2,3), \tag{5·2}$$

where
$$W(\phi_s) = -\pi i\int_0^{i\infty} H_\nu^{(1)}(kr)\,H_\nu^{(1)}(kr')\,e^{i\nu\pi}\cos\nu(\pi-|\phi_s-\theta|)\,d\nu, \tag{5·3}$$

https://doi.org/10.1017/S0305004100041815 Published online by Cambridge University Press

$$D_j = -\pi i \int_0^{i\infty} H_\nu^{(1)}(kr)\, H_\nu^{(1)}(kr')\, e^{i\nu\pi} \sin \nu\pi\, P_j\, d\nu \quad (j = 1, 2, 3), \tag{5·4}$$

and the reflexion coefficients

$$\begin{aligned} B_s^j &= (-1)^{sj} \quad \text{for} \quad j = 1, 2, \\ &= (-1)^{\mu_s} \quad \text{for} \quad j = 3. \end{aligned} \tag{5·5}$$

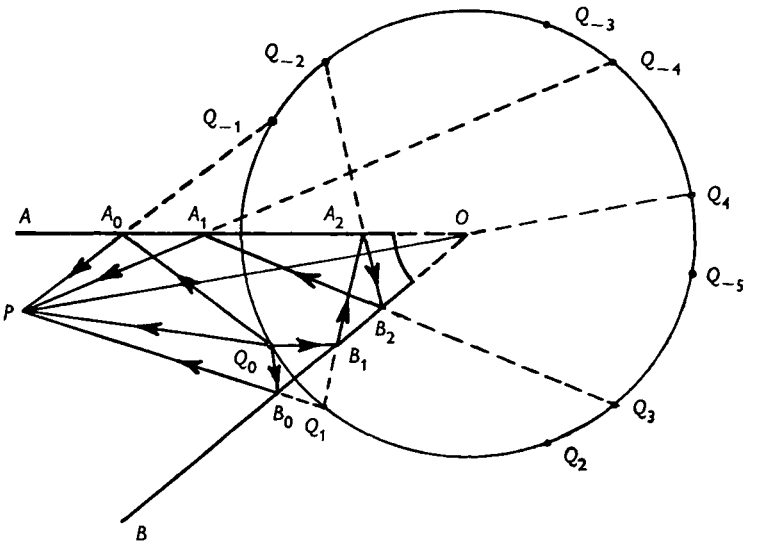


Fig. 2. The direct and various reflected waves form the plane boundaries.

Since we have taken the incident field as $\pi i\, H_0^{(1)}(kR)$, where

$$H_0^{(1)}(kR) = -\int_0^{i\infty} H_\nu^{(1)}(kr)\, H_\nu^{(1)}(kr')\, e^{i\nu\pi} \cos \nu(\pi - |\phi - \theta|)\, d\nu, \tag{5·6}$$

$$R^2 = r^2 + r'^2 - 2rr' \cos(\phi - \theta), \tag{5·7}$$

we get

$$W(\phi_s) = \pi i\, H_0^{(1)}(kR_s), \tag{5·8}$$

where

$$R_s^2 = r^2 + r'^2 - 2rr' \cos(\phi_s - \theta). \tag{5·9}$$

Evidently, for $s = 0$, R_0 will be the shortest distance between the source and the observer. Here in Figure 2, $R_0 = Q_0 P$ is the path of the incident wave at P due to a source at Q_0. For other values of Q_s the location of ϕ_s are such that R_s can always be broken up satisfying the laws of reflexion at the plane boundaries, in a suitable form. As, for example, $R_1 = Q_1 P = Q_0 B_0 + B_0 P$ and $R_{-1} = Q_{-1} P = Q_0 A_0 + A_0 P$ are the paths for once reflected waves. However, $R_1 \neq R_{-1}$ in general. Again,

$$R_4 = PQ_{-4} = Q_0 B_1 + B_1 A_2 + A_2 B^2 + B_2 A_1 + A_1 P$$

is the path for the four-times reflected waves.

We see clearly that s coincides exactly with the number of reflexions on either of the two plane boundaries. Further, we know before hand the number of times of reflexion of the reflected wave generated by an imaginary source $Q_s(r', \phi_s)$. Only $Q_0(r', \phi)$ will correspond to the actual line source inside the medium. One important

https://doi.org/10.1017/S0305004100041815 Published online by Cambridge University Press

restriction on ϕ_s is $0 < \phi_s < 2\pi$. Further, for positive s the sources are situated in $0 < \phi_s < \pi + \theta$ and for negative s in $\pi - \theta < \phi_s < 2\pi$. These conditions may be obtained from the convergency of the integrals on infinite arcs (cf. Hudson (4)). Thus, we have seen that for a given value of α and (r', ϕ) the whole image system is fixed and the process of finding the reflected path is as follows: Join the observing point to any given imaginary source; then the line joining them will intersect with either of the straight lines $\theta = 0$ or $\theta = \alpha$ at the point say A_s or B_s. Now as long as the above condition is satisfied by a given observing point in relation to an imaginary source, another imaginary source spaced at equal angular distance in reference to the straight lines $\theta = 0$ or $\theta = \alpha$ (which one has been intersected) will be found. Join this imaginary source with A_s or B_s as the case may be and then this line will interesect $\theta = \alpha$ or $\theta = 0$ at B_{s-1} or A_{s-1} (say) and the whole process is repeated s times until it converges to Q_0, the actual source in the physical medium. But on the contrary if the above condition is violated, then at some step the process will fail and we shall not get an imaginary source spaced at equal angular distance from either of the two plane boundaries and the process will not converge to Q_0. This may be verified from Figure 2, by choosing two observing points P_1 and P_2 in the regions $\angle POA$ and $\angle POB$ respectively where the condition $\phi_4 < \pi + \theta$ will be violated in the first case and satisfied in the second case. Thus, the complete geometry of the reflected wave having only reflexion at the plane boundaries, i.e. the rays from the imaginary sources not touching or cutting the cylinder may be found in this way.

6. *Evaluation of the 'shadow zone of the images'.* It should be noted that since the apex is removed by a circular cylinder, all the sources $Q_{\pm s}$ cannot contribute to disturbances at P in general. Particularly the rays from the imaginary sources which will cut or touch the cylinder cannot reach the observing point by mere reflexion. In section 5 the term I_j^P (cf. (3·23) and (3·36)) has been considered to analyse the field due to reflexion at the sides without meeting the cylinder. Let $\bar{I}_j^P$ denote the terms of I_j^P when $P_j(\nu)$ is subtracted from $F_j(\nu)$ and expressed in the form

$$\bar{I}_j^P = \sum_s B_s^j I_j^{PS},$$

where

$$I_j^{PS} = i \int_0^{i\infty} H_\nu^{(1)}(kr)\, H_\nu^{(1)}(kr')\, e^{i\nu\pi} \cos \nu(\pi - \phi_s + \theta)\, d\nu.$$

Clearly, $-\pi I_j^{PS} = W(\phi_s)$ (cf. (5·3)), is the field due to the s-time reflected wave at the plane boundaries. Now as $|s|$, the number of reflexion increases, the point of intersection of the straight line joining the image source (r', ϕ_s) and the observing point (r, θ) with the line $\theta = 0$ or $\theta = \alpha$, moves towards the apex of the complete wedge. The question naturally arises what should be the role of I_j^{PS} when the point of intersection falls inside the cylinder, i.e. either on OA' or OB' (cf. Figure 4)? These waves cannot reach the point P by mere reflexion in our case. We shall show in section 8 that this term will correspond to the diffracted wave at the cylinder. To facilitate this, we shall search for another suitable representation of I_j^{PS} corresponding to the ray which has intersection either at some point on OA' or OB'. In this article we shall show that in fact there exists a representation of I_j^{PS} (cf. (6.13)) in terms of I_j^{QS}, I_j^{RS} (cf. (6·11) and (6·12)) and two line integrals $\mathscr{L}_1$, $\mathscr{L}_2$ (cf. (6·8) and (6·10)) all of which will involve the

https://doi.org/10.1017/S0305004100041815 Published online by Cambridge University Press

parameter a, the radius of the cylinder, as we expect it, in a certain restricted region; because in this region only $\mathscr{L}_1$, $\mathscr{L}_2$ will be convergent. To find the required restriction mathematically we shall consider the short-wave approximation using appropriate asymptotic expansion of $H_\nu^{(1)}(z)$. These have been discussed by Striefer and Kodis (**10**, **11**) recently. They have shown that for asymptotic values of $H_\nu^{(1)}(z)$, $H_\nu^{(2)}(z)$, $J_\nu(z)$ the complex ν-plane can be broken up in the following regions as shown in Figure 3 and these

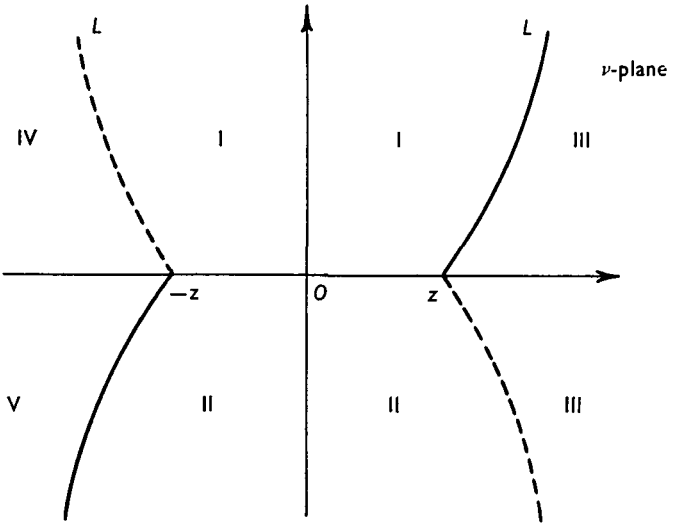


Fig. 3. The different region for the asymptotic expression of the cylindrical functions.

are continuous functions of ν so long as these curves are not crossed. The thick line curve separating the regions I and III or II and V are the curves on which the zeros $H_\nu^{(1)}(z)$ and $dH_\nu^{(1)}/dz$ will lie. In the regions I and II

$$H_\nu^{(1)}(z) \approx \left(\frac{2}{\pi}\right)^{\frac{1}{2}} \frac{\exp i\{(z^2-\nu^2)^{\frac{1}{2}} - \nu\cos^{-1}(\nu/z) - \frac{1}{4}\pi\}}{(z^2-\nu^2)^{\frac{1}{4}}} + O(z^{-1}), \tag{6·1}$$

$$H_\nu^{(2)}(z) \approx \left(\frac{2}{\pi}\right)^{\frac{1}{2}} \frac{\exp i\{-(z^2-\nu^2)^{\frac{1}{2}} + \nu\cos^{-1}(\nu/z) + \frac{1}{4}\pi\}}{(z^2-\nu^2)^{\frac{1}{4}}} + O(z^{-1}), \tag{6·2}$$

$$J_\nu(z) \approx \left(\frac{2}{\pi}\right)^{\frac{1}{2}} \frac{\cos\{(z^2-\nu^2)^{\frac{1}{2}} - \nu\cos^{-1}(\nu/z) - \frac{1}{4}\pi\}}{(z^2-\nu^2)^{\frac{1}{4}}} + O(z^{-1}) \quad \text{(near the real axis)} \tag{6·3}$$

$$\approx (2\pi)^{-1} \frac{\exp\{\pm i[(z^2-\nu^2)^{\frac{1}{2}} - \nu\cos^{-1}(\nu/z) - \frac{1}{4}\pi]\}}{(z^2-\nu^2)^{\frac{1}{4}}} + O(z^{-1})$$

$$\text{(far from the real axis)}, \tag{6·4}$$

where the upper sign refers to the region I and the negative sign that for II and also

$$|\arg(z^2-\nu^2)^{\frac{1}{2}}| < \tfrac{1}{2}\pi, \quad 0 < \Re(\cos^{-1}\nu/z) \leqslant \pi, \tag{6·5}$$

$$\Im\{\cos^{-1}\nu/z\} = \begin{cases} < 0 & \text{in I,} \\ = 0 & \text{in the boundary,} \\ > 0 & \text{in II.} \end{cases} \tag{6·6}$$

https://doi.org/10.1017/S0305004100041815 Published online by Cambridge University Press

Now choose a contour Γ_3 in the region I (Figure 3) such that it runs:

(i) from $i\infty$ to $0+$, along the imaginary axis;

(ii) from 0 to ka along the real axis, the zeros of $\sin \nu\pi$ being half-encircled by semi-circles and the origin by a quarter of a circle;

(iii) along the line $\widehat{ZL}$, the zeros of $H_\nu^{(1)}(ka)$ being encircled by part of a circle; and

(iv) closed by a portion of a circle of large radius.

Hence performing the integration

$$\int_{\Gamma_3} \frac{J_\nu(ka)}{H_\nu^{(1)}(ka)} H_\nu^{(1)}(kr) H_\nu^{(1)}(kr') \frac{\cos \nu(\pi - \phi_s + \theta)}{\sin \nu\pi} d\nu \tag{6·7}$$

we get

$$\int_{i\infty}^{0} Q_\nu \frac{\cos \nu(\pi - \phi_s + \theta)}{\sin \nu\pi} d\nu - \pi i \sum_{m=0}^{M} \frac{\epsilon_m J_m(ka)}{H_m^{(1)}(ka)} H_m^{(1)}(kr) H_m^{(1)}(kr') \cos m(\phi_s - \theta)$$
$$+ \int_0^{ka} Q_\nu \frac{\cos \nu(\pi - \phi_s + \theta)}{\sin \nu\pi} d\nu - \pi i \sum_{n=1}^{\infty} \frac{J_{\nu_n}(ka)}{\partial/\partial\nu [H_{\nu_n}^{(1)}(ka)]_{\nu=\nu_n}}$$
$$\times H_{\nu_n}^{(1)}(kr) H_{\nu_n}^{(1)}(kr') \frac{\cos \nu_n(\pi - \phi_s + \theta)}{\sin \nu_n \pi} + \mathscr{L}_1 = 0, \tag{6·8}$$

where $\mathscr{L}_1$ is the line integral along $\widehat{ZL}$. Q_ν and ϵ_m are defined in (3·17) and (3·19) respectively. Also here m is an integer and M is the number of zeros of $\sin \nu\pi$ between 0 and ka. Clearly, so long as $0 < \phi_s - \theta < 2\pi$ the integrals converge on the large circle. Similarly we integrate

$$\int_{\Gamma_4} \frac{J_{-\nu} e^{i\nu\pi}}{H_\nu^{(1)}(ka)} H_\nu^{(1)}(kr) H_\nu^{(1)}(kr') \frac{\cos \nu(\pi - \phi_s + \theta)}{\sin \nu\pi} d\nu, \tag{6·9}$$

where Γ_4 is a contour in second quadrant of the complex ν-plane and it runs:

(i) from $i\infty$ to $0+$, along the imaginary axis;

(ii) along the real negative axis, from $0-$ to $-ka$, zeros of $\sin \nu\pi$ being encircled by semi-circles and the origin by a quarter of a circle;

(iii) along the dotted curve $-ZL'$;

(iv) closed by a portion of large circle;

we get,

$$\int_{i\infty}^{0} Q_{-\nu} \frac{\cos \nu(\pi - \phi_s + \theta)}{\sin \nu\pi} d\nu - \pi i \sum_{m=0}^{M} \frac{\epsilon_m J_m(ka)}{H_m^{(1)}(ka)} H_m^{(1)}(kr) H_m^{(1)}(kr') \cos m(\phi_s - \theta)$$
$$+ \int_0^{-ka} Q_{-\nu} \frac{\cos \nu(\pi - \phi_s + \theta)}{\sin \nu\pi} d\nu + \mathscr{L}_2 = 0, \tag{6·10}$$

where $\mathscr{L}_2$ is the integral along the dotted curve. By giving a similar definition as in (3·14), (3·16), (3·25) and (3·26) and subtracting (6·10) from (6·8) we get

$$I_j^{PS} - \tfrac{1}{2} L_j^S + \mathscr{L}_1 - \mathscr{L}_2 = 0 \quad (j = 1, 2, 3), \tag{6·11}$$

where the additional S in the index denotes that, instead of $F_j(\nu)$ we are writing here $\cos \nu(\pi - \phi_s + \theta)/\sin \nu\pi$ (compare (3·1) and (3·17)). Also, it is evident from (6·10) that

https://doi.org/10.1017/S0305004100041815 Published online by Cambridge University Press

by changing ν to $-\nu$ in $\int_0^{-ka}$, the integral becomes identical with $\int_0^{ka}$. Again using a similar definition as in (3·34) we get

$$L_j^S = -I_j^{PS} - 2I_j^{QS} + 2I_j^{RS}. \tag{6·12}$$

Therefore

$$I_j^{PS} = \tfrac{2}{3}(I_j^{RS} - I_j^{QS}) - \tfrac{2}{3}(\mathscr{L}_1 - \mathscr{L}_2) \tag{6·13}$$

provided that line integrals $\mathscr{L}_1$ and $\mathscr{L}_2$ are finite. Using the asymptotic values of (6·1) through (6·4) it can be shown that the integrands on $\mathscr{L}_1$ and $\mathscr{L}_2$ are of the form

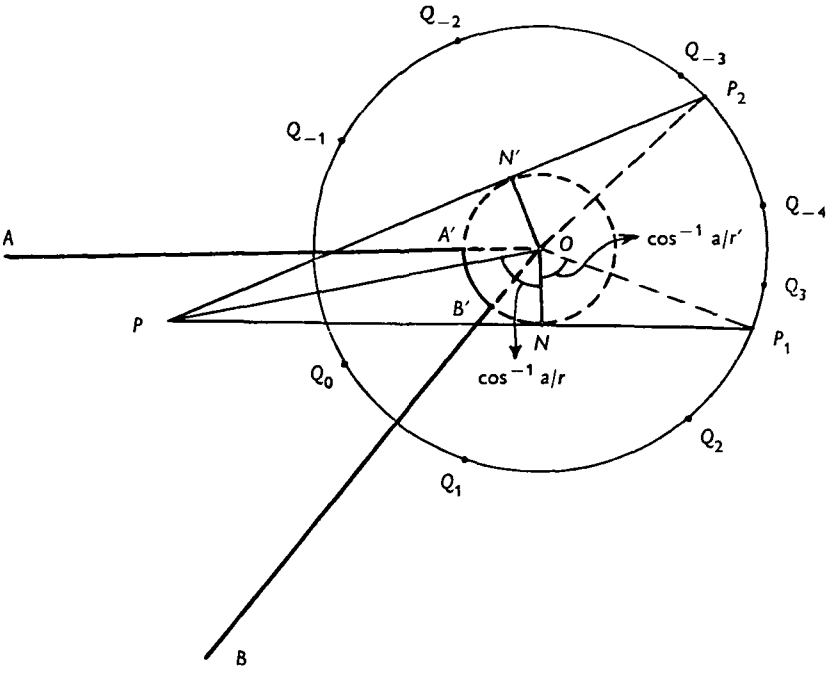


Fig. 4. 'Shadow zone of the images', relative to an observer.

$\chi(\nu)\, e^{i\zeta(\nu)}$ (cf. (7·7)). Hence to find the convergency of the line integral (i.e. in that case the integrals will be finite) we note that

$$\Im\,\zeta(\nu) > 0 \quad \text{as} \quad |\nu| \to \infty \quad \text{along } ZL \text{ and } -ZL' \quad \text{(cf. Figure 3)}, \tag{6·14}$$

which gives after a little calculation

$$\phi_s - \theta > \cos^{-1}\frac{a}{r} + \cos^{-1}\frac{a}{r'}$$

and

$$2\pi - \phi_s + \theta < \cos^{-1}\frac{a}{r} + \cos^{-1}\frac{a}{r'},$$

i.e. the region

$$\phi_{s_1} < \phi_s < \phi_{s_2}, \tag{6·15}$$

where

$$\phi_{s_1} = \cos^{-1}\frac{a}{r} + \cos^{-1}\frac{a}{r'} + \theta \tag{6·16}$$

and

$$\phi_{s_2} = 2\pi - \cos^{-1}\frac{a}{r} - \cos^{-1}\frac{a}{r'} + \theta. \tag{6·17}$$

https://doi.org/10.1017/S0305004100041815 Published online by Cambridge University Press

Clearly, (6·15) gives the 'shadow zone of the images' relative to the observing point P due to the cylindrical obstacle, i.e. any image which will fall in $P_1\hat{O}P_2$ (on the other side of P) will not send any reflected wave at P. As a matter of fact these rays would have at least the final reflexion from either some point on OA' or OB' if the surface $\widehat{A'B'}$ was absent.

7. *Reflected waves from the cylindrical boundary.* The last two terms of (3·36) can be written as

$$2\pi\left[\int_{i\infty}^{0}+\int_{0}^{\infty} Q_\nu F_j(\nu)\,d\nu\right]. \tag{7·1}$$

If we set apart the terms containing P_j (cf. (4·17)) from (7·1) we get

$$2\pi\sum_{s=-m}^{m-1} B_s^j\left[\int_{i\infty}^{0}+\int_{0}^{\infty}\left\{\frac{J_\nu(ka)}{H_\nu^{(1)}(ka)}H_\nu^{(1)}(kr)\,H_\nu^{(1)}(kr')\frac{\cos\nu(\pi-\phi_s+\theta)}{\sin\nu\pi}\right\}d\nu = I_j^{RC}+I_j^{RS} \quad (j=1,2,3), \tag{7·3}$$

where

$$I_j^{RC} = 2\pi i\sum_{s=-m}^{m-1} B_s^j\left[\int_{i\infty}^{0}+\int_{0}^{\infty}\left\{\frac{H_\nu^{(2)}(ka)}{H_\nu^{(1)}(ka)}H_\nu^{(1)}(kr)\,H_\nu^{(1)}(kr')\,e^{-i\nu\pi}\cos\nu(\pi-|\phi_s-\theta|)\,d\nu\right\}\right] \tag{7·4}$$

and to obtain I_j^{RS}, $J_\nu(ka)$ in (7·3) is to be replaced by $J_{-\nu}(ka)\,e^{-i\nu\pi}$. For the geometrical interpretation of the term I_j^{RC}, we shall evaluate it by the method of steepest descent. The path for the steepest descent may be obtained by writing out the asymptotic expansion of the Hankel functions as described in (6·1)–(6·6). Since the second and fourth quadrants will not contain any of the singularities, the integral on the positive imaginary axis and real axis may be transformed to a suitable path Γ_s as shown in Figure 5, for a fixed value of s (for a similar contour, cf. Keller and Karal (6)). The end of the saddle-path Γ_s should not cross the dotted curve in Figure 3 because on the other part $H_\nu^{(1)}(z)$, $H_\nu^{(2)}(z)$ will increase exponentially.

If we write

$$f(\Phi_s) = \int_{\Gamma_s}\frac{H_\nu^{(2)}(ka)}{H_\nu^{(1)}(ka)}H_\nu^{(1)}(kr)\,H_\nu^{(1)}(kr')\,e^{-i\nu\Phi_s}d\nu, \tag{7·5}$$

then
$$I_j^{RC} = \sum_{0}^{m-1}\pi i B_s^j[f(\phi_s-\theta)+f(2\pi-\phi_s+\theta)] + \sum_{1}^{m}\pi i\,B_{-s}^j[f(2\pi-\phi_{-s}+\theta)+f(\phi_{-s}-\theta)]. \tag{7·6}$$

Using (6·1) and (6·2), (7·5) can be written as

$$f(\Phi_s) = \int_{\Gamma_s}\chi(\nu)\,e^{i\zeta(\nu)}d\nu, \tag{7·7}$$

where

$$\zeta(\nu) = \sqrt{(k^2r^2-\nu^2)}+\sqrt{(k^2r'^2-\nu^2)}-2\sqrt{(k^2a^2-\nu^2)} - \nu\left[\cos^{-1}\frac{\nu}{kr}+\cos^{-1}\frac{\nu}{kr'}-2\cos^{-1}\frac{\nu}{ka}+\Phi_s\right], \tag{7·8}$$

$$\chi(\nu) = (2\pi)^{-1}e^{-\frac{1}{2}i\pi}(k^2r^2-\nu^2)^{-\frac{1}{4}}(k^2r'^2-\nu^2)^{-\frac{1}{4}}. \tag{7·9}$$

https://doi.org/10.1017/S0305004100041815 Published online by Cambridge University Press

The saddle-point of the integrand of (6·7) is $\nu = \nu_s$, where ν_s is the root of $\zeta'(\nu_s) = 0$. The form (7·8) suggests that for different values of s for a suitable observing point extremum values of ν_s occur when $\nu_{s_m} = \pm ka$, i.e. for $\nu = \nu_{\pm s_m}$

$$\cos^{-1}\frac{a}{r} + \cos^{-1}\frac{a}{r'} - \Phi_{s_m} = 0 \quad \text{for} \quad \nu_{s_m} = ka$$

and

$$\cos^{-1}\frac{a}{r} + \cos^{-1}\frac{a}{r'} - \Phi_{-s_m} = 0 \quad \text{for} \quad \nu_{s_m} = -ka.$$

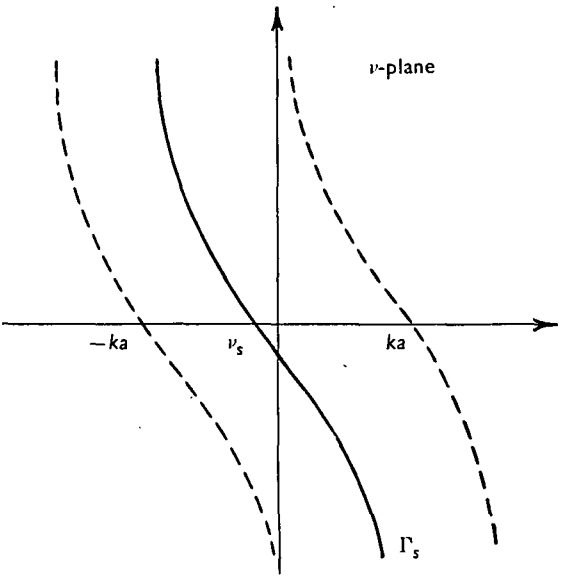


Fig. 5. Path of steepest descent for the integrals. Dotted curves are the two extremum positions.

Thus the phase term $\zeta(\nu)$ in both the cases becomes

$$k[\sqrt{(r^2 - a^2)} + \sqrt{(r'^2 - a^2)}].$$

Geometrically this means that the source (r', ϕ_{s_m}) will send grazing rays at the surface $r = a$ to the observing point. In Figure 6

$$PC'_{-3} = \sqrt{(r^2 - a^2)},$$

$$Q_{-3}C'_{-3} = \sqrt{(r'^2 - a^2)},$$

$$\phi_{-3} = 2\pi - \angle POC'_{-3} - \angle C'_{-3}OQ_{-3} - \angle POA_2.$$

Also, $PC'_{-3} = PA_2 + A_2B_1 + B_1C_3$ and $C'_{-3}Q_{-3} = Q_2C'_3 = C_3A_1 + A_1Q_0$.

In the physical domain these rays will correspond to the rays which will go a total number of s_m times of reflexion at either of the plane boundary and in the course it will touch $r = a$ once at (a, β) when $0 < \beta < \alpha$ (cf. Figure 6).

The roots of $\zeta'(\nu) = 0$ are given by

$$\sin^{-1}\frac{\nu}{kr} + \sin^{-1}\frac{\nu}{kr'} - 2\sin^{-1}\frac{\nu}{ka} - \Phi_s = 0, \tag{7·10}$$

https://doi.org/10.1017/S0305004100041815 Published online by Cambridge University Press

where $$-\tfrac{1}{2}\pi < \sin^{-1}\nu/z < \tfrac{1}{2}\pi \quad \text{(cf. (6·5) and } z = kr, kr', ka). \tag{7·11}$$

(7·10) may be satisfied by the substitution

$$\nu_s = kr\sin\xi_s = kr'\sin\xi_s' = ka\sin\lambda_s, \tag{7·12}$$

where ξ_s, ξ_s', λ_s will be connected by a relation. For the first integral of (7·6) we note that the saddle-point occurs at $\nu = -\bar{\nu}_s$ and then combining (7·10) and (7·12)

$$\bar{\xi}_s + \bar{\xi}_s' + \phi_s - \theta = 2\bar{\lambda}_s \tag{7·13}$$

is well satisfied by the geometric construction (cf. quadrilateral OPC_2Q_1O in Figure 7), satisfying laws of reflexion. For the second term of (7·6) saddle-points occur for

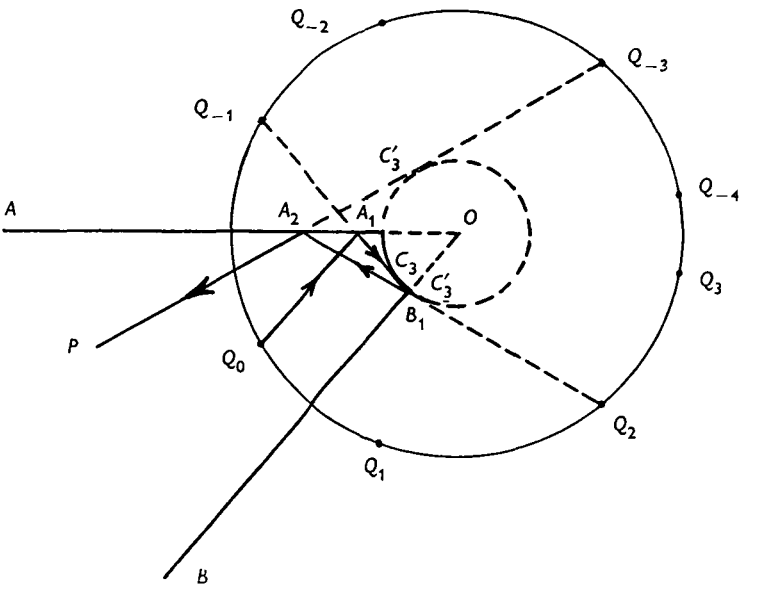


Fig. 6. Geometry of a grazing ray. Each reflected wave will touch the cylinder either in the real or imaginary part.

positive ν_s but redefining the angle ξ_s, ξ_s' and λ_s we shall get the same contribution for fixed s ($s \geqslant 0$). This is further corroborated by the fact that $\phi_s - \theta$ and $2\pi - \phi_s + \theta$ are interior and exterior angles at O for a given (r, θ) and (r', ϕ_s) ($s \geqslant 0$). Similar arguments hold for the last two terms of (7·6) since the extremum saddle-paths pass through $\pm ka$ we see that ϕ_s is bounded and

$$0 < \phi_s \leqslant \phi_{s_1}, \quad \phi_{s_2} \leqslant \phi_s < 2\pi, \tag{7·14}$$

where ϕ_{s_1} and ϕ_{s_2} are given by (6·16) and (6·17). Sign of the equality will hold in the favourable circumstances. This shows that the shadow zone of the images for the wave having reflexion at the cylindrical boundary is the same as before.

Evaluating (7·6)

$$I_j^{RC} = -\sum_s 2B_s^j \left(\frac{\pi}{2k}\right)^{\frac{1}{2}} \left[\frac{a\cos\lambda_s}{\zeta_s r'\cos\xi_s + \zeta_s' r\cos\xi_s'}\right]^{\frac{1}{2}} \times \exp\left[ik(\zeta_s + \zeta_s')\right] \quad (0 < \phi_s \leqslant \phi_{s_1},\ \phi_{s_2} \leqslant \phi_s < 2\pi), \tag{7·15}$$

https://doi.org/10.1017/S0305004100041815 Published online by Cambridge University Press

where
$$\zeta_s = r\cos\xi_s - a\cos\lambda_s, \tag{7·16}$$

$$\zeta_s' = r'\cos\xi_s' - a\cos\lambda_s. \tag{7·17}$$

The meaning of ζ_s and ζ_s' are evident. The extra negative sign in the reflexion coefficient B_s^j appears due to the assumption that $r = a$ is a rigid boundary. Note that $B_s^j = B_{-s}^j$ holds for $j = 1, 2$ but not for $j = 3$, which is due to the different conditions on the plane boundaries for $j = 3$ (Hudson's case). If we allow the change in the reflexion coefficient for the plane boundary as -1 for Dirichlet's condition and 1 for the Neumann's condition then a little calculation will show that B_s^j gives the correct value of reflexion

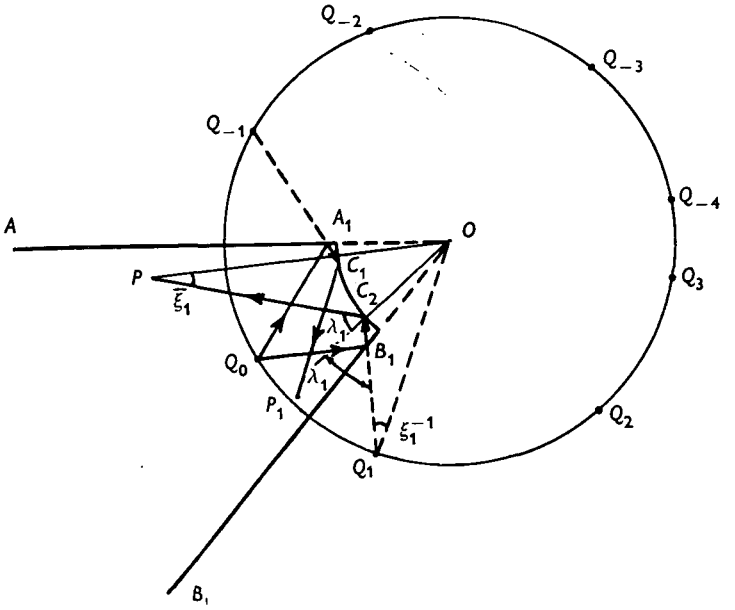


Fig. 7. Reflected waves at the cylindrical boundary.

coefficient for s-multiply reflected wave for all the cases for $j = 1, 2, 3$. One may compare the divergence coefficient obtained here with that of the complete rigid cylinder (cf. Gilbert(3)). For a geometrical picture two cases are to be distinguished, (a) when the incident wave from $Q_{\pm s}$ ($s \neq 0$) and ϕ_s satisfies (7·14) hits at (a, β) and $0 < \beta < \alpha$, i.e. inside the physical domain (Figure 7). Here $\zeta_1' = C_2Q_1$ can be broken up as $Q_0B_1 + B_1C_2$ and $\zeta_1 = C_2P$ will be unchanged. (b) When the incident wave from $Q_{\pm s}$ will hit $r = a$ outside the physical domain say at (a, β') ($\alpha < \beta' < \theta + \cos^{-1}a/r$ and $0 < 2\pi - \beta' < \cos^{-1}a/r - \theta$ (cf. Figure 8)). Here both ζ_s and ζ_s' are to be broken up, clearly $\zeta_2 = C_2P = C_1B_1 + B_1P$ and with a little geometry $\zeta_2' = Q_2C_2 = Q_0A_1 + A_1C_1$. Similar reductions are possible for all other paths.

8. *Diffracted waves at the cylindrical boundary.* In sections 5–7 we have discussed the entire reflected field and showed that for $0 < \phi_s < \phi_{s_1}$ and $\phi_{s_2} < \phi_s < 2\pi$, reflexion occurs. In this section we shall show that the image lying in the region $\phi_{s_1} < \phi_s < \phi_{s_2}$

https://doi.org/10.1017/S0305004100041815 Published online by Cambridge University Press

will produce diffracted waves. Let in this region $\bar{G}_j$ be the field when P_j is set apart from $F_j(\nu)$, then from (3·36), (4·17) and (4·22)

$$\bar{G}_j = \sum_s B_s^j G_j^s, \tag{8·1}$$

where
$$G_j^s = -\pi I_j^{PS} - 2\pi I_j^{QS} + 2\pi I_j^{RS} \quad (j = 1, 2, 3). \tag{8·2}$$

I_j^{PS}, I_j^{QS} and I_j^{RS} are already defined in section 6 and B in (5·5). Since, in the region $\phi_{s_1} < \phi_s < \phi_{s_2}$
$$I_j^{PS} = \tfrac{2}{3}(I_j^{RS} - I_j^{QS}) - \tfrac{2}{3}(\mathscr{L}_1 - \mathscr{L}_2).$$

Therefore
$$G_j^S = \tfrac{4}{3}\pi(I_j^{RS} - I_j^{QS}) + \tfrac{2}{3}\pi(\mathscr{L}_1 - \mathscr{L}_2). \tag{8·3}$$

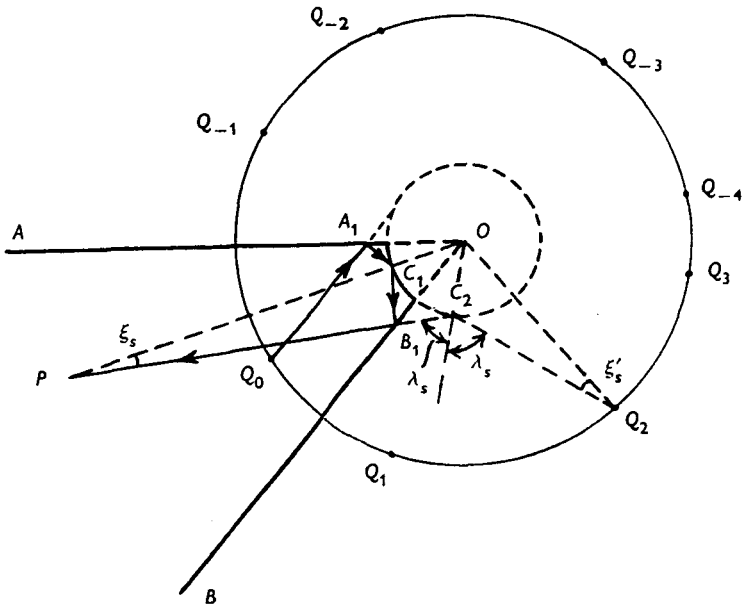


Fig. 8. Reflected waves at the cylindrical boundary.

But since the integrals $\mathscr{L}_1$ and $\mathscr{L}_2$ are unknown we shall use the alternative form of G_j^S which is obtained by substituting (6·13) in (6·12) and comparing it with (8·3) and noting also that $G_j^S = \pi L_j^S$ we get

$$G_j^S = \pi^2 i \sum_{n=1}^{\infty} \frac{H_{\nu_n}^{(2)}(ka)}{\partial/\partial\nu[H_{\nu_n}^{(1)}(ka)]_{\nu=\nu_n}} H_{\nu_n}^{(1)}(kr)\, H_{\nu}^{(1)}(kr') \frac{\cos\nu_n(\pi - \phi_s + \theta)}{\sin\nu_n\pi}$$

which facilitates the ray-picture. Therefore,

$$\bar{G}_j = \pi^2 i \sum_s \sum_{n=1}^{\infty} B_s^j \frac{H_{\nu_n}^{(2)}(ka)}{\partial/\partial\nu[H_{\nu}^{(1)}(ka)]_{\nu=\nu_n}} H_{\nu_n}^{(1)}(kr)\, H_{\nu_n}^{(1)}(kr') \frac{\cos\nu_n(\pi - \phi_s + \theta)}{\sin\nu_n\pi} \quad (\phi_{s_1} < \phi_s < \phi_{s_2}). \tag{8·4}$$

Now we write for large ka using (2·6)

$$\nu_n = ka + i\eta_n, \tag{8·5}$$

$$\eta_n = \sqrt{3}/4(ka)^{\frac{1}{3}}[\tfrac{3}{4}\pi(4n-1)]^{\frac{2}{3}} \tag{8·6}$$

https://doi.org/10.1017/S0305004100041815 Published online by Cambridge University Press

neglecting the term containing $(ka)^{\frac{1}{3}}$ in the real part of ν_n. Also since $\eta_n > 0$ we have

$$\frac{e^{-i\eta_n\pi}}{\sin\nu_n\pi} = -2i\sum_{l=0}^{\infty} e^{2il\nu_n\pi}. \tag{8·7}$$

Thus (8·4) becomes

$$\pi^2 \sum_{s>s_1}^{s<s_3} \sum_{l=0}^{\infty} \sum_{n=1}^{\infty} B_s^j \frac{e^{-\eta_n q_s}}{D(\nu_n)} e^{ikp_s}, \tag{8·8}$$

where

$$p_s = \sqrt{(r^2-a^2)} + \sqrt{(r'^2-a^2)} + aq_s, \tag{8·9}$$

$$q_s = \Phi_s - \cos^{-1}\frac{a}{r} - \cos^{-1}\frac{a}{r'} + 2l\pi, \tag{8·10}$$

$$\Phi_s = \phi_s - \theta, \quad \text{or} \quad 2\pi - \phi_s + \theta \tag{8·11}$$

and

$$D(\nu) = (\tfrac{1}{2}\pi)^{\frac{1}{2}} e^{\frac{1}{4}i\pi}\, \partial/\partial\nu[H_\nu^{(1)}(ka)]\,[(k^2a^2-\nu^2)\,(k^2r^2-\nu^2)\,(k^2r'^2-\nu^2)]^{\frac{1}{4}}. \tag{8·12}$$

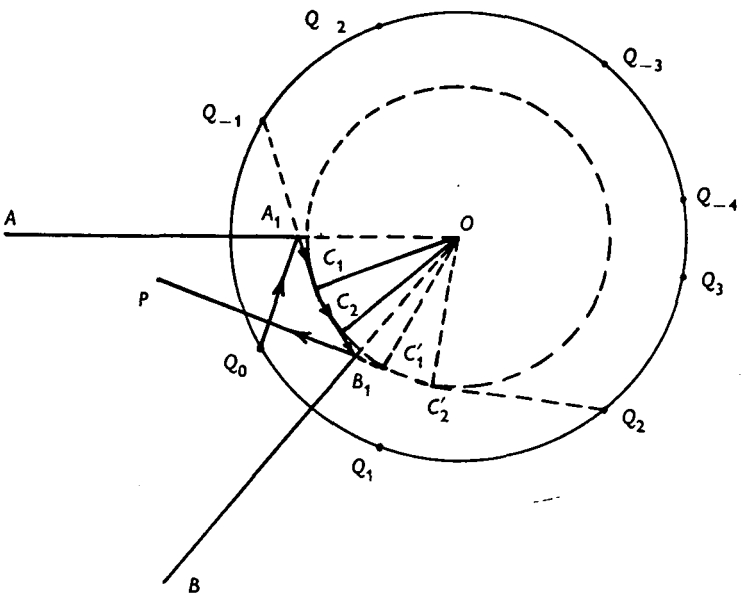


Fig. 9. Diffracted wave at the cylindrical boundary.

Either $\partial/\partial\nu[H_\nu^{(1)}(ka)]_{\nu=\nu_n}$ can be computed bringing the Airy function in the usual way or the following expression can be used near $\nu = \nu_n$

$$H_\nu^{(1)}(ka) \approx 2i\left(\frac{2}{\pi}\right)^{\frac{1}{2}} \frac{\sin\{(k^2a^2-\nu^2) - \nu\cos^{-1}(\nu/ka) - \frac{1}{4}\pi\}}{(k^2a^2-\nu^2)^{\frac{1}{4}}}. \tag{8·13}$$

In the above figure for the observer P, Q_2 falls in the shadow zone of the images (i.e. if we draw two tangents from P to the circle $r = a$ of Figure 9, $Q_2, Q_3, \ldots, Q_{-3}$ fall inside that angle). Hence the phase term p_2 becomes

$$p_2 = \sqrt{(r^2-a^2)} + \sqrt{(r'^2-a^2)} + a\phi_2 - a\left(\cos^{-1}\frac{a}{r} + \cos^{-1}\frac{a}{r'} + \theta + 2l\pi\right).$$

https://doi.org/10.1017/S0305004100041815 Published online by Cambridge University Press

Here $$C_1'P = \sqrt{(r^2-a^2)}, \quad C_2'Q_2 = \sqrt{(r'^2-a^2)},$$

$$\angle C_1OC_2 = \angle C_1'OC_2' = \phi_2 - \cos^{-1}\frac{a}{r} - \cos^{-1}\frac{a}{r'} - \theta.$$

Clearly, $C_1'P = PB_1 + B_1C_2$ and $C_2'Q_2 = C_1Q_{-1} = Q_0A_1 + A_1C_1$ (proof of which is not difficult). Diffraction occurs once only on the surface of the cylinder $r = a$ at $\widehat{C_1C_2}$ for $l = 0$, due to the image source ϕ_2. Again the rays for $l > 0$ correspond to the rays which move along the boundary for several times and reach P in the favourable circumstances. One important fact is to be noted from (8·8) and (8·10) that practically the whole contribution will be obtained even when l and n are not very far from 1. This also decreases with r and r' as can be seen from (8·12).

9. *Scattered waves due to various parts of the medium.* Comparing (3·36) and (4·17) we note that the three integrals in (3·36) containing P_j can be combined to write as

$$\pi^2 i \sum_{n=1}^{\infty} \frac{H_{\nu_n}^{(2)}(ka)}{\partial/\partial\nu[H_\nu^{(1)}(ka)]_{\nu=\nu_n}} H_{\nu_n}^{(1)}(kr)\, H_{\nu_n}^{(1)}(kr')\, P_j(\nu_n) \quad (j = 1, 2, 3). \tag{9·1}$$

If $\alpha = \pi/m$ for $j = 1, 2$ and $\alpha = \pi/2m$ for $j = 3$, (9·1) vanishes. Apart from these terms we have also I_j^{RS} ($0 < \phi_s < \phi_{s_1}$, $\phi_{s_2} < \phi_s < 2\pi$; cf. (7·4)) where its counterpart I_j^{RC} (in $0 < \phi_s < \phi_{s_1}$, $\phi_{s_2} < \phi_s < 2\pi$) has been explained as the total reflected field at the cylindrical boundary. On the real axis part of I_j^{RS}, $J_{-\nu}(ka)$ may be replaced by $\cos\nu\pi\,\mathrm{Ai}(q) + \sin\nu\pi\,\mathrm{Bi}(q)$ (cf. Striefer and Kodis(10)) where $\mathrm{Ai}(q)$ and $\mathrm{Bi}(q)$ are Airy functions. From the foregoing discussion it is seen that we have obtained (i) direct wave, (ii) reflected waves due to the plane boundaries, (iii) reflected waves due to the cylindrical boundary, (iv) diffracted waves at the cylindrical boundary. But the scattered waves due to the two apexes has not been obtained. We therefore guess that these unaccounted terms may be explained in terms of scattering. We are not persevering in estimating these scattering terms due to two reasons. (*a*) Scalar wave solution will get little application in seismology, and (*b*) the time-dependent part should not be taken harmonic to keep the physical nature of the problem.

10. *Conclusion.* The propagation of *SH*-waves due to a line source in the convex part of the medium formed by a circular cylinder of arbitrary radius and two planes has been considered. The image sources have been exactly located and expressed in a single formula and hence the consideration of the reflexion and diffraction of the multiple phases are possible.

Here only either Dirichlet or Neumann's condition has been used on $r = a$, but mixed boundary conditions may be used with constant or variable impedance, since the condition of orthogonality still holds. But in that case the path Γ_s for the steepest descent will have to cross a certain pole in suitable circumstances and the first motion of the creeping waves along the boundary can be determined (cf. Keller and Karal(6), Kane(5)). Further, the method suggests that the deviation from $r = a$ is possible satisfying similar orthogonality relation (2·11). The solution for the three-dimensional case for point source is possible and can be obtained after a manner indicated by Oberhettinger(8), for the case of acoustic waves, etc., where no coupling occurs with other kinds of wave.

https://doi.org/10.1017/S0305004100041815 Published online by Cambridge University Press

I wish to express my thanks to Dr S. C. Das Gupta for suggesting the investigation and to the referee for his valuable suggestions and critical comments for improvement of the paper.

APPENDIX A

Case I. If $\alpha = \pi/m$ and m be an even integer, from equation (4·5)

$$\sum_{l=1}^{m} \cos\nu\left[\pi - \frac{2\pi}{m}(l-1) - \Phi_1\right] = \sum_{l=0}^{\frac{1}{2}m-1} \cos\nu\left[\pi - \frac{2\pi l}{m} - \Phi_1\right] + \sum_{1}^{\frac{1}{2}m} \cos\nu\left[\pi - \left\{2\pi - \frac{2\pi l}{m}\right\} - \Phi_1\right]. \quad \text{(A 1)}$$

Clearly, the right-hand side of (A 1) may be written as

$$\sum_{l=0,2,4,\ldots}^{m-2} \cos\nu\left[\pi - \frac{\pi l}{m} - \Phi_1\right] + \sum_{l=1,3,5,\ldots}^{m-1} \cos\nu\left[\pi - \left\{2\pi - \left(\frac{\pi l}{m} + \frac{\pi}{m}\right)\right\} - \Phi_1\right]. \quad \text{(A 2)}$$

Similarly,

$$\sum_{l=1}^{m} \cos\nu\left[\pi - \frac{2\pi l}{m} + \Phi_2\right] = \sum_{l=1,3,5,\ldots}^{m-1} \cos\nu\left[\pi - \left(\frac{\pi l}{m} + \frac{\pi}{m}\right) + \Phi_2\right] + \sum_{l=0,2,4,\ldots}^{m-2} \cos\nu\left[\pi - \left\{2\pi - \frac{\pi l}{m}\right\} + \Phi_2\right]. \quad \text{(A 3)}$$

Hence

$$\begin{aligned}\sin\nu\pi\, F_j(\nu) = {} & \sum_{l=0,2,4,\ldots}^{m=2} \cos\nu\left[\pi - \frac{\pi l}{m} - \Phi_1\right] + (-1)^j \sum_{l=1,3,5,\ldots}^{m-1} \cos\nu\left[\pi - \left\{\frac{\pi l}{m} + \frac{\pi}{m}\right\} + \Phi_2\right] \\ & + (-1)^j \sum_{l=0,2,4,\ldots}^{m-2} \cos\nu\left[\pi - \left\{2\pi - \frac{\pi l}{m}\right\} + \Phi_2\right] \\ & + \sum_{l=1,3,5,\ldots}^{m-1} \cos\nu\left[\pi - \left\{2\pi - \left(\frac{\pi l}{m} + \frac{\pi}{m}\right)\right\} - \Phi_1\right] \\ & (\Phi_1, \Phi_2 \text{ are given by (2·22)}). \quad \text{(A 4)}\end{aligned}$$

For $\theta < \phi$ the four summations in (A 4) can be written as (4·6). For $\theta > \phi$ (A 2) is to be slightly modified. If m be an odd integer then instead of breaking up the summation from 1 to $\frac{1}{2}m$ and $\frac{1}{2}m$ to m as in (A 1) we have to reduce it to 1 to $\frac{1}{2}(m-1)$ and $\frac{1}{2}(m+1)$ to m. For $j = 3$ a similar proof may be constructed.

Case II. If $\pi/m < \alpha < \pi/(m-1)$ the equality of the two summations of (4·4) will not hold good and therefore a modification is necessary. Applying (4·1)

$$\frac{\sin\nu\pi\, \cos\nu(\alpha - \Phi)}{\sin\nu\alpha} = \sum_{l=1}^{n} \cos\nu[\pi - 2(l-1)\alpha - \Phi] + \sum_{l=1}^{n} \cos\nu[\pi - 2l\alpha + \Phi] + \frac{\sin\nu(\pi - 2n\alpha)\cos\nu(\alpha - \Phi)}{\sin\nu\alpha}. \quad \text{(A 5)}$$

https://doi.org/10.1017/S0305004100041815 Published online by Cambridge University Press

If m be an even integer equal to $2n$ then for $\Phi = \Phi_1$, and Φ_2 we shall use (A 5). If $m = 2n+1$ then for $\Phi = \Phi_1$ we shall replace n by $n+1$ in (A 5) and for $\Phi = \Phi_2$ keep (A 5) unchanged. Hence if m be an even integer and $\theta < \phi$

$$\begin{aligned}\sin \nu\pi F_j(\nu) = &\sum_{l=1}^{n} \cos \nu[\pi - 2(l-1)\alpha - \phi + \theta] + \sum_{l=1}^{n} \cos \nu[\pi - 2l\alpha + \phi - \theta] \\ &+ (-1)^j \sum_{l=1}^{n} \cos \nu[\pi - 2(l-1)\alpha - \phi - \theta] \\ &+ (-1)^j \sum_{l=1}^{n} \cos \nu[\pi - 2l\alpha + \phi + \theta] + P_j \sin \nu\pi, \end{aligned} \tag{A 6}$$

P_j is given by (4·20). Using

$$\cos \nu(\pi - \Phi - \theta) = \cos \nu[\pi - (2\pi - \Phi) + \theta]$$

(A 6) may be written as

$$\begin{aligned}\sin \nu\pi\, F_j(\nu) = &\sum_{l=1}^{n} \cos \nu(\pi - \phi_l^{(1)} + \theta) + (-1)^j \sum_{l=1}^{n} \cos \nu(\pi - \phi_l^{(2)} + \theta) \\ &+ (-1)^j \sum_{l=1}^{n} \cos \nu(\pi - \phi_l^{(3)} + \theta) \\ &+ \sum_{l=1}^{n} \cos \nu(\pi - \phi_l^{(4)} + \theta) + P_j \sin \nu\pi \quad (j = +1, 2), \end{aligned} \tag{A 7}$$

where

$$\left.\begin{aligned}\phi_l^{(1)} &= 2(l-1)\alpha + \phi, \\ \phi_l^{(2)} &= 2\pi - [2(l-1)\alpha + \phi], \\ \phi_l^{(3)} &= 2l\alpha - \phi, \\ \phi_l^{(4)} &= 2\pi - (2l\alpha - \phi). \end{aligned}\right\} \tag{A 8}$$

Selecting $\phi_1^{(1)}$ as ϕ_1, $\phi_1^{(3)}$ as ϕ_2, $\phi_2^{(1)}$ as ϕ_3, $\phi_2^{(3)}$ as ϕ_4 and so on..., and $\phi_1^{(2)}$ as ϕ_{-1}, $\phi_1^{(4)}$ as ϕ_{-2} and so on we shall get the required result (4·17). However (A 7) may be expressed in a similar form as in (A 4). If m be an odd integer the modification is possible and P_j will be given by (4·21). For $\theta > \phi$ labelling of the angles in (A 8) should be rearranged. For $j = 3$, a similar proof may be constructed but care should be taken for the presence of the factor of the type $(-1)^l$ in each summation.

REFERENCES

(1) COHEN, D. S. *Comm. Pure Appl. Math.* **17** (1964), 23.
(2) DUWALO, G. and JACOBS, J. A. *Canad. J. Phys.* **37** (1959), 109.
(3) GILBERT, F. *J. Acoust. Soc. Amer.* **32** (1960), 841.
(4) HUDSON, J. A. *Geophys. J.* **7** (1963), 1.
(5) KANE, J. *Div. Eng. Res. Dev.* (1960), reprint no. 26.
(6) KELLER, J. B. and KARAL, F. C. *J. Appl. Phys.* **31** (1960), 1039.
(7) MACDONALD, H. M. *Proc. London Math. Soc.* **26** (1895), 156.
(8) OBERHETTINGER, F. *Comm. Pure Appl. Math.* **7** (1954), 551.
(9) SOMMERFELD, A. *Partial differential equation in physics* (Academic Press; New York, 1949).
(10) STRIEFER, W. and KODIS, R. D. *Quart. Appl. Math.* **21** (1964), 285.
(11) STRIEFER, W. and KODIS, R. D. *Quart. Appl. Math.* **23** (1965), 27.

https://doi.org/10.1017/S0305004100041815 Published online by Cambridge University Press